ASIA TURBOMACHINERY & PUMP SYMPOSIUM
SINGAPORE | 22 – 25 FEBRUARY 2016
MARINA BAY SANDS

Centrifugal Compressor Surge Control Systems - Fundamentals of a Good Design

Kamal Botros, PhD, PEng
Research Fellow
NOVA Chemicals
Calgary, AB, Canada

Kamal is a Research Fellow of Fluid Dynamics with NOVA Chemicals. He has been with the company since 1984. Over the past 38 years he has worked on various fluid flow and equipment dynamic problems related to oil and gas processing and transportation facilities, as well olefins and polyolefins manufacturing processes. He is well published (198 papers, 2 books and 4 patents) all related to industrial applications and issues.

Steven Hill, PE
Sr. Mechanical Engineer
Williams Gas Pipeline
Houston, TX, USA

Steven earned a Bachelor of Science in Mechanical Engineering from the University of Texas at San Antonio. He began his career at NASA serving as a flight controller in mission control, and later as the active thermal control system project engineer for the Orion Program manned space capsule.

Since 2008, Steven has focused on the design, installation and commissioning of modular and stick-built oil refineries and gas processing plants in North America, Africa, Asia and the Middle East. In his most recent role, he has supported the design, installation, and commissioning of numerous compressor installations on the Williams Transco pipeline network.

Jordan Grose, PEng
Manager, Vibration Integrity Group
BETA Machinery Analysis
Calgary, AB, Canada

Jordan is a mechanical engineer with a wide range of domestic and international design, field, and monitoring experience with compressors, pumps, piping, and other production machinery. He has specialized skills in vibration, performance, and troubleshooting in onshore and offshore production facilities. Jordan has been with BETA Machinery Analysis (BETA) for the last 12 years, during which time he has authored and co-authored several papers. He was formerly responsible for BETA's Malaysia office in Kuala Lumpur.

Jordan currently leads BETA's Vibration Integrity Group in addressing plant wide vibration risks in piping and machinery systems. The group addresses client's integrity needs by identifying vibration risks in production assets, and systematically mitigating those risks with engineering analyses through to practical solutions. The goal of the Vibration Integrity Group is to increase the value of production assets by preventing and mitigating failures due to vibration.

ABSTRACT

Many facilities employ two or more centrifugal compressors, operated in either series or parallel configurations. An accurately designed surge control system that includes multiple compressors with the associated piping systems is a vital element of a facility's design and ongoing operational integrity. The design must ensure compressors are not subjected to damaging fast dynamic events leading to large capital costs and significant down time for operators. Examples of such fast dynamic events are those following emergency shutdown (ESD) or fast stop of one or all compressor units in a station. Typical studies are not accurate enough to capture the complex interactions leading to catastrophic events, especially for complicated system arrangements.

This paper introduces three methods of surge control analysis that can be conducted to assess the effectiveness of any surge control system design to prevent the compressor from surge. The first method utilizes the perturbation theory to relate the compressor deceleration and the resulting drop in its flow and head to determine the elapsed time that the compressor can stay out of surge before the surge control system brings about enough positive flow to prevent the unit from undergoing deep surge. The second method is simpler, and is based on a dimensionless number, called the inertia number, which combines the salient parameters from the dynamic equation between the fluid energy and that of the compressor rotor inertia to determine, as a first cut check, if the surge control system is adequate. The third method, which is always recommended, and is based on solving the full gas dynamic

partial differential equations (PDEs) in spatial and temporal domain, which describe the true dynamic characteristics of the flow through the various piping elements, the compressor itself, to provide much more accurate predictions of surge control system behavior during fast transient events.

Comparisons are made to field measurements to provide model validations, and an example application (Case Study) of three units operating in parallel. The first two (Units 6 and 7) were existing in a compressor station, while the third (Unit 8) was an add-on. The addition of Unit 8 meant a number of station layout modifications, which included: re-wheeling of Units 6 and 7 (i.e., change the compressor impellers); adding after gas cooling; and relocating the anti-surge valves downstream of the coolers to allow for both hot (fast stop) and cold recycle (anti-surge) capabilities. Due to the addition of equipment and significant reconfiguration of station piping and valves, a dynamic surge analysis on Units 6, 7, and 8 was required to determine whether the existing anti-surge and fast stop valves were adequately sized and whether the anti-surge valves could be relocated downstream of the gas coolers. A new fast stop recycle system was added along with Unit 8, which also needed to be adequately sized. Further complications arose from the fact that Unit 6's anti-surge valve configuration differs from that of Unit 7 and that Unit 6 has twin recycle valves jointly serving as anti-surge valves with a single fast stop valve while Unit 7 has a single anti-surge valve and a single fast stop valve.

NOMENCLATURE

A - *pipe cross-section area*
c - *speed of sound*
c_1 - *speed of sound at suction condition*
c_2 - *speed of sound at discharge condition*
C_v - *gas specific heat at constant volume*
D - *pipe internal diameter*
D_o - *impeller outer (tip) diameter.*
D_i - *impeller average inlet diameter.*
E - *friction and heat transfer source term in the energy equation*
f_{DW} - *Darcy-Weisbach friction factor*
g - *acceleration of gravity*
H_o - *compressor head at steady state point*
H_a - *compressor adiabatic head at any given inlet flow (Q_a)*
H_z - *compressor adiabatic head at zero flow*

$$= \alpha \sum_{1}^{n} U_i^2$$

H_s - *compressor head at surge point at the current running speed.*
I - *compressor/driver combined inertia*
k - *isentropic exponent of the gas*
$\dot{m}$ - *gas mass flow rate through the compressor*
N - *compressor speed*
N_I - *inertia number*
P - *pressure*
P_1 - *suction static pressure*
P_2 - *discharge static pressure*
Q - *flow*
Q_a - compressor actual inlet flow.
Q_s - *compressor actual inlet flow at surge point at the same speed.*
R - *gas constant*
t - *time*
T - *gas temperature*
T_a - *surrounding (ambient) temperature*
T_1 - *suction gas temperature*
u - *gas mean flow velocity*
U_h - *overall heat transfer coefficient between fluid and surrounding*
U_i - *rotational tip velocity of impeller (i).*
x - *spatial length along a pipe*
$(\ )_v$ - *derivative at constant volume*
$(\ )_s$ - *derivative at constant entropy*
Z_{av} - *average gas compressibility factor*
α - *zero flow head coefficient (equal to 1.0 for loss free impeller, and approx. equal to 0.4-0.6 to account for losses).*
β - *friction and elevation source term in the momentum equation*
γ - *parameter = 0.5 (H_s-H_o)*
ϕ - *thermodynamic derivative (dimensionless)*
η_a - *compressor adiabatic efficiency*
η_m - *mechanical efficiency*
ρ_1 - *gas density at compressor inlet*
ρ - *gas density*
τ – *pre-stroke delay plus pressure wave arrival time*

INTRODUCTION

Compression systems are employed in almost every stage of gas production, processing, transportation, storage, and distribution facilities. They provide a vital function to the overall operation of these systems, and therefore, must be vigilantly monitored in order to ensure a high level of operational reliability. The majority of these compression systems employ centrifugal compressors, in either single- or multi-staged arrangements depending on the pressure ratio requirements. They are driven by either gas turbines or electric motors with/without gearboxes. These compression systems are required to not only withstand uninterrupted operation for extended periods of time, but also be able to cope with flow and pressure transients associated with part-load operation, startup and emergency shutdown (ESD) [1-8].

During these transients, the centrifugal compressor may come close to or cross the surge limit, which could drive the compressor into deep surge, a violent instability that often damages the compressor itself, its bearing, seal, rotor assembly, and casing. Anti-surge systems are therefore employed to be activated to prevent the unit for undergoing surge. These anti-surge systems (or surge control systems) consist of one or two recycle lines around the compressor, which are equipped with fast acting valves that open when the compressor approaches the surge limit. When this happens, the compressor(s) interacts dynamically with system components around them, i.e. piping, fittings and equipment, drivers [9-10]. Additionally, surge control logic and associated controller parameter tuning process play important roles in the overall dynamics during ESD or fast stop of the compressor [11].

Fluid inertias and compressor/driver rotor inertias play an important role in either stabilizing or destabilizing the system dynamics [12]. The compressors' performance characteristics also have an important role in the system dynamics behavior [13]. Ensuring reliable and safe operation of the various aspects of these compression systems requires a wholesome understanding of their dynamic behavior, which enables good system design, operation, and control.

Several experimental and numerical investigations aimed at analyzing the dynamic interactions that take place between compression system components, particularly during ESD, have been reported, e.g., [14-18]. In these investigations, the surge model proposed by Greitzer and Moore [19,20] has been extended to centrifugal compressors. The method of characteristics for the solution of the governing one-dimensional equations of gas flow [21] has been proven to be adequate and correlates well with field measurements [13].

The modern surge control design process often involves analyses using the "lumped parameter" method of solving system ordinary differential equations (ODEs) which describe the gas dynamics, equipment, and control responses during a transient event. The lumped parameter method facilitates the selection of suitable components for a particular surge control system, or assesses the performance of an existing one. While this method provides reasonable approximations for simplified systems, it does not produce accurate representations for complex installations having several dissimilar compressors connected in parallel and series through complex suction and discharge piping systems. For such systems, a better approach is required to accurately assess the surge characteristics of the system and how the compressors interact, and to protect the machinery from unexpected dynamic behaviors.

The present paper describes three methods for determining the effectiveness of any specific recycle system and recycle valve characteristics. These three methods are: i) a simplified method based on system impedance, ii) the concept of the Inertia number and iii) full dynamic simulation of the compression system.

FAST DYNAMIC EVENTS ASSOCIATED WITH ESD OR FAST STOP PROCESSES

Of particular concern are the dynamics that occur following ESD, fast stop or power failure, as they represent the most severe and fast transients that could cause damage to the compressor unit and surrounding equipment. Parameters that affect the potential for the compressor to undergo surge during ESD are the recycle system gas volume, recycle valve characteristics such as maximum capacity, flow vs. opening characteristics, opening delay (i.e. the time between valve open solenoid drop out and the start of the valve stem movement on the valve – often called 'pre-stroke' delay), and valve travel time (i.e. the time taken for the valve to travel from closed to open positions – often called 'stroke' time) [15,16]. Additionally, timing of the compressor ESD signal, the fuel gas shutoff signal, fuel gas manifold size (in the case of gas turbine drivers), power train inertia, and the compressor's aerodynamic characteristics close to the surge point, all contribute to the complexity of the problem [12,13,17,18].

In the case of high pressure ratio (high head) multi-stage compressors, after coolers (typically aerial type) are often employed to bring the discharge gas temperature down to a level accepted for continuous operation of the downstream process and piping (set by the external coating maximum temperature limit). Two recycle systems are then contemplated: a) a single recycle system where the recycle path includes the aerial cooler as shown in Fig. 1 (top); and b) a dual recycle system where in addition to the aforementioned recycle system, another short-circuited system is employed specifically to deal with compressor surge control, as shown in Fig. 1 (bottom). In the dual recycle system, the longer recycle system is often called the cold recycle, as it re-circulates cooler gas downstream of the aerial cooler back to the compressor suction. The shorter recycle system is also called a hot recycle system for the opposite reason.

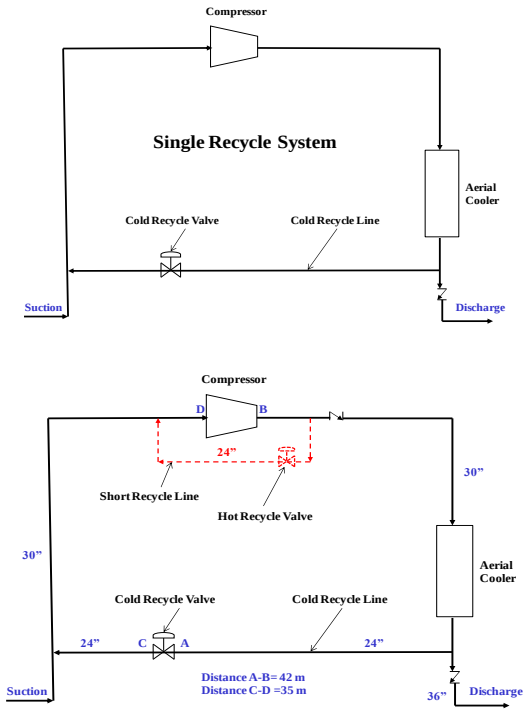

Figure 1: Single vs. Dual Recycle Systems.

The process of compressor station ESD is schematically depicted on a head-flow diagram in Fig. 2, following a trend observed both experimentally and numerically [12-14]. Six phases are identified as the compressor decelerates from a steady state point (S.S.) to zero flow and zero head across the compressor. Following an ESD, the operating point of the compressor follows approximately a straight line characterized by the slope (*S*) for a period of time before any expansion or pressure waves arrive at the compressor outlet or inlet, respectively, as a result of opening the recycle valve. This period corresponds to the recycle valve pre-opening (pre-stroke) delay, which is a combined effect of a process signal delay and inherent mechanical delay in opening of the recycle valve once an ESD signal is issued. During this phase (Phase I), although the driver power is assumed to be completely shut-off, the compressor continues to rotate due to the combined inertia of its shaft, impeller and driver. The compressor decelerates due to the head across it, windage, friction, etc., according to the balance of the following equation:

$$\dot{W}_{driver} = I_{driver} \cdot N_{driver} \cdot \frac{dN_{driver}}{dt} + I_c \cdot N_c \cdot \frac{dN_c}{dt} + \frac{\dot{m} H_a}{\eta_a \eta_m} + Windage\ \&\ Losses \quad (0)$$

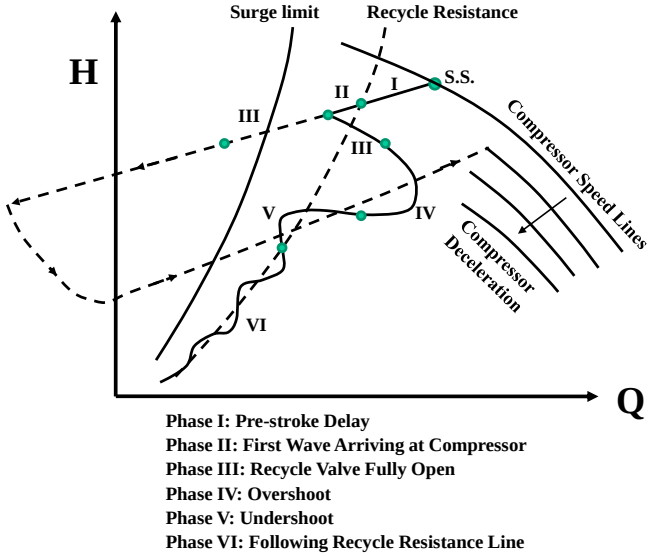

Figure 2: Schematic of the Various Phases of an ESD Process Tracked on a Compressor Performance Characteristics Chart (Wheel Map).

In the above equation, it is assumed that the driver power was set to zero instantaneously at the instant of ESD. While this is correct for cases where electric motors are used as drivers, it is not absolutely correct for cases with gas turbine drivers. White and Kurz [17] have shown that one of the key problems is that there is residual power from the gas turbine even after the fuel is shut off. This is due to two effects: one is that there is always some fuel gas remaining in the fuel gas manifold system which will continue to feed the gas turbine combustor and hence sustain power for a few hundred milliseconds; and secondly, the rotor inertia of the gas generator itself will continue to provide hot gas to the power turbine even at a decreasing temperature. These effects can be mathematically represented by describing the power term on the left hand side of Eq. (0), $\dot{W}_{driver}$, as a declining function of time instead of setting it to zero at the instant of ESD. Similar treatment can be adopted to steam turbine drivers.

Once the recycle valve opens, a pressure wave travels downstream of the valve along the low pressure part of the recycle line and along the main suction line, while an expansion wave travels upstream of the valve along the high pressure part of the recycle line and along the main discharge line. The first wave to arrive at the compressor suction or discharge sides depends on the distance which either wave needs to travel, and the local speed of sound along the corresponding path. The time taken for either wave to arrive first to the compressor determines the duration of Phase II shown in Fig. 2. Once this wave arrives at the compressor, the

flow starts to increase through the compressor and head decreases, and hence the beginning of Phase III. The slope of the characteristic line shown in Fig. 2 ($S=dH/dQ$), can be determined from the perturbation theory since small pressure perturbation is related to local velocity perturbation by the characteristic impedance of the gas on either side of the compressor, that is:

On the suction side of the compressor:

$$\delta P_1 = -\frac{\rho_1 c_1}{A_1}\delta Q \tag{1}$$

and on the discharge side:

$$\delta P_2 = \frac{\rho_2 c_2}{A_2}\left(\frac{\rho_1}{\rho_2}\right)\delta Q = \frac{\rho_1 c_2}{A_2}\delta Q \tag{2}$$

Following the expression of the isentropic head in terms of the pressure ratio across the compressor in the form:

$$H = \xi\left[\left(\frac{P_2}{P_1}\right)^{\frac{k-1}{k}} - 1\right] \tag{3}$$

$$where:\ \xi = \frac{Z_{av}RT_1}{\left(\frac{k-1}{k}\right)}$$

The perturbation in H is related to the perturbation of P_1 and P_2 at a given operating condition corresponding to compressor head (H_o) in the form:

$$\delta H = \left(\frac{k-1}{k}\right)(H_o + \xi)\left[\frac{\delta P_2}{P_2} - \frac{\delta P_1}{P_1}\right] \tag{4}$$

The slope (S) can then be determined from Eqs. 1, 2 and 4 as follows:

$$S = \frac{dH}{dQ} = \left(\frac{k-1}{k}\right)(H_o + \xi)\left[\frac{\rho_1 c_1}{P_1 A_1} + \frac{\rho_1 c_2}{P_2 A_2}\right] \tag{5}$$

In Equation (5) above, when all parameters are in SI units, the units of the slope S will be (J.s/kg.m^3). The recycle valve continues to open to the maximum open position resulting in further pressure waves and expansion waves arriving at the compressor suction and discharge sides, respectively. However, due to gas inertia in the recycle line and mainline, the flow through the compressor tends to overshoot as is manifested by Phase IV, followed by a short period of undershoot (Phase V) around the recycle system resistance line shown in Fig. 2. The final Phase VI is compressor wind down in which small over- and under-shootings around the recycle system resistance line occur until zero flow and zero head are reached. Note that the recycle system resistance line is not the surge control line [21,22].

In the next Section, three methods are described that provide a basis for assessing the effectiveness and responsiveness of a given surge control system for a given compression train. These three methods vary in their complexity, whereby method III, which is based on solving the full governing dynamic equation in spatial and temporal domains, being the most complex but most comprehensive and accurate.

EVALUATION OF THE RECYCLE SYSTEM DYNAMICS DURING ESD

Three methods will be applied here to assess the present surge protection system when an emergency shutdown (ESD) or fast stop is initiated. These methods are:

- Method I: Impedance Characteristics
- Method II: Inertia Number
- Method III: Full Dynamic Simulations.

Method I: Impedance Characteristics

The basis for the impedance characteristics method follows the perturbation relationship between head and flow derived in the previous section, resulting from the initial reduction in flow through the compressor and the deceleration of the compressor rotor due to the exchange of the energy between the gas and the compressor rotor. If surge is to be prevented, the maximum allowable drop in the compressor speed before the arrival of either the first expansion wave to arrive at the compressor discharge flange or the compression wave to arrive at the compressor suction flange, both resulting from opening of the closest recycle valve, can be determined by running a tangent from the initial operating point with an impedance characteristics slope 'S' to the compressor characteristic at speed (No - δN_{max}), as shown in Fig. 3. If the compressor speed drops below this limiting speed during ESD operation (as a result of e.g., low compressor inertia, an initial condition of high head, a late arrival of the first expansion wave to the compressor discharge or the pressure wave to the suction of the compressor), the compressor will undergo reverse flow (surge). This is because the compressor impeller at speeds slightly lower than (No - δN_{max}) cannot sustain a positive flow against the prevailing high differential pressure

(head) across it. In this case, the high differential pressure will drive reverse flow through the impeller while it is spinning forward. This is defined by the intersection of the characteristic line with the full compressor characteristic at the prevailing speed at this instant (point B in Fig 3), hence the development of the first surge cycle.

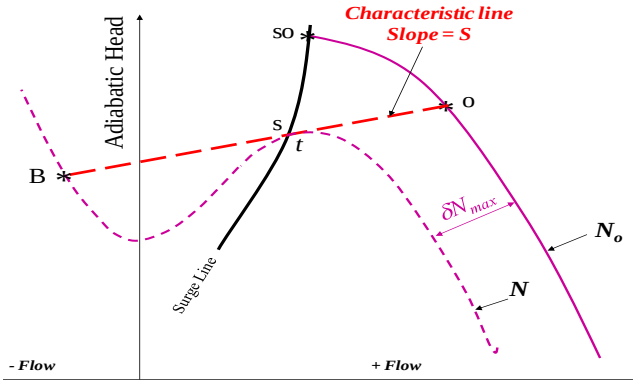

Figure 3: Determination of the Maximum Drop in Compressor Speed and Hence δt_{max} Before Compressor Surging upon ESD.

In summary:

if $\delta N > \delta N_{max}$, surge will occur, and
if $\delta N < \delta N_{max}$, surge will not occur.

Here, δN is determined from ESD equation (0), which can be simplified for the case of gas turbine driven compressors as follows:

$$-I\,N_o \cdot \frac{dN}{dt} = \frac{\dot{m}_o\,H_o}{\eta_a\,\eta_m} \tag{6}$$

Theoretically, if the characteristic slope 'S' is known, and the initial condition of the compressor (point 'o') is known, the maximum speed drop can be determined from geometrical algebra established by Fig. 3 and the fan laws of the compressor characteristics, including the cubic representation of the full compressor characteristics to the left of the surge point [20]. One approximation is to assume that (N_o - δN_{max}) corresponds to the mainline characteristics line meeting the compressor speed line at the surge point (s) at speed = N_o - δN_{max} instead of being tangent to it at point (t) as shown in Fig. 3. This approximation is, in fact, more realistic as the surge point (s) defines the surge limit. Following the fan laws the relation between adiabatic heads, actual inlet flows, and compressor speeds at surge points can be correlated as follows:

$$\frac{Q_s}{N} = \frac{Q_{so}}{N_o} = K_1\ ; \qquad \frac{H_s}{N^2} = \frac{H_{so}}{N_o^2} = K_2 \tag{7}$$

According to the above discussion and referring to Fig. 3, the following relation can be written:

$$S = \frac{H_o - H_s}{Q_o - Q_s} \tag{8}$$

where 'S' is the slope of the characteristic line defined by Eq. (5).

Introducing Eq. (7) into Eq. (8), the following equations can be developed:

$$\begin{aligned} H_o - H_s &= S\left(Q_o - Q_s\right) \\ H_o - K_2\left(N_o - \delta N\right)^2 &= S\left[Q_o - K_1\left(N - \delta N\right)\right] \\ H_o - K_2 N_o^2 + 2K_2 N_o \delta N &= S\left[Q_o - K_1 N_o + K_1 \delta N\right] \\ H_o - H_{so} + 2H_{so}\frac{\delta N}{N_0} &= S\left[Q_o - Q_{so} + Q_{so}\frac{\delta N}{N_o}\right] \end{aligned} \tag{9}$$

and finally,

$$\frac{\delta N_{\max}}{N_o} = \frac{S\left(Q_o - Q_{so}\right) + \left(H_{so} - H_o\right)}{2H_{so} - S\,Q_{so}} \tag{10}$$

Now combining Eq. (10) and Eq. (6) and integrating, we arrive at the simple equation that determines the maximum (longest) time that the compressor can withstand before going into surge, i.e., before the arrival of the relief expansion or pressure waves resulting from opening the recycle valve, as follows:

$$\delta t_{\max} = I\,N_o^2\left[\frac{S\left(Q_o - Q_{so}\right) + \left(H_{so} - H_o\right)}{2H_{so} - S\,Q_{so}}\right] / \left[\frac{\dot{m}_o\,H_o}{\eta_a\,\eta_m}\right] \tag{11}$$

The above equation, though simple and easy to evaluate, is significant. The $\delta t_{\max}$ thus calculated by this equation can be compared to the time it will take for the first relief expansion or pressure wave to arrive at the compressor discharge or suction side, respectively. This time of arrival can be estimated from the sum of the recycle valve pre-stroke delay

and the travel time of either the expansion or the pressure wave to arrive at the compressor. The latter is calculated from the distance along the corresponding piping between the recycle valve and the compressor and the local speed of sound in the gas, either on the discharge or the suction side, respectively.

Figure 4 shows an example of head-flow characteristics of a high head compressor unit employed in a natural gas compression system depicted schematically in Fig. 1 (bottom).

The compressor is driven by aero-derivative gas turbine. A steady state operating point was assumed close to the surge control line as shown in Fig. 4 at Q_o = 4.363 m^3/s and H_o = 37.072 kJ/kg. Other relevant parameters required for the calculation of $\delta t_{\max}$ in Eq. (11) are given in Table 1. The resulting $\delta t_{\max}$ is calculated as 115 ms. According to the axial distances along the suction and discharge piping separating the cold recycle valve from the compressor (see Fig. 1-bottom), the arrival time of the expansion and pressure waves, along with valve pre-stroke delay are calculated in Table 2. These times are 296 ms and 288 ms, respectively. Clearly, the compressor in this case will undergo surge following an ESD operation since the time of arrival of either wave is much longer than $\delta t_{\max}$ of 115 ms calculated above. In fact, the pre-stroke delay alone of this valve (=200 ms) is obviously too long to prevent the compressor unit from surging.

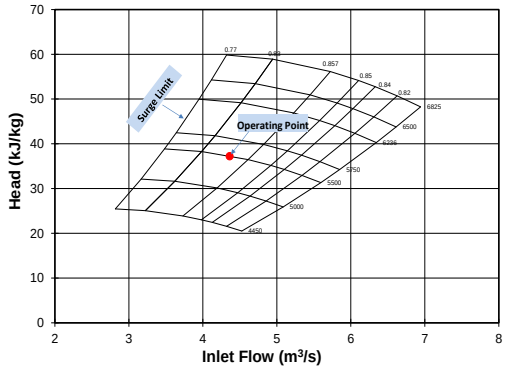

Figure 4: Method I Example: Compressor Characteristics and Initial Operating Condition.

A field test of a fast stop at much lower speed and head was conducted on this compressor. At the time of the test, only the cold recycle was installed. The results of this test is shown in Fig. 5 and indicate that the compressor has undergone several surge cycles as it was winding down following the fast stop. The initial steady state operating point for this test was Q_o = 3.0 m^3/s and H_o = 22.5 kJ/kg. Other relevant parameters required for the calculation of $\delta t_{\max}$ in Eq. (11) are given in Table 2. Again, the compressor in this case has undergone surge following a fast stop since the time of arrival of either wave is much longer than $\delta t_{\max}$ of 102 ms calculated in Table 3.

The obvious solution is not only to employ a recycle valve that has a shorter pre-stroke delay, but to have it located very close to either compressor discharge (preferable) or suction sides. This means, a dual recycle system is required, i.e., the addition of a short (hot) recycle system as shown in Fig. 1-bottom (dotted line). Again, the function of the short recycle system is for surge protection during ESD or fast stop, while the cold recycle system which includes the aerial cooler in the recycle path, is for unit startup and part load operation. A hot recycle was subsequently sized and installed around this compressor, and another field test was performed from an initial condition shown in Fig. 6 and Table 3. Test results are also shown in Fig. 6 indicating that the compressor was driving toward surge but, due to the close proximity of the hot recycle to the compressor discharge (5 m on the discharge side) and that the hot recycle valve pre-stroke delay was shortened to 120 ms, the compressor was prevented from going into deep surge. The corresponding Method I calculations for this case are given in Table 4 showing $\delta t_{\max}$ = 125 ms, and time for the arrival of the first expansion wave to the compressor discharge flange is 131.88 ms (Table 5).

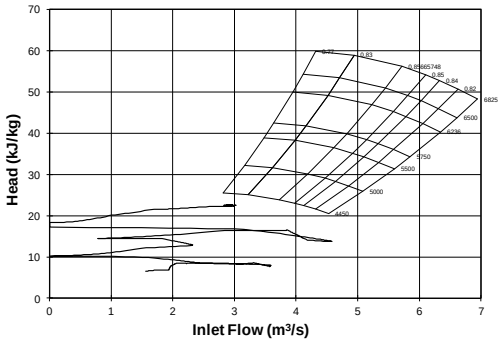

Figure 5: Field Measurements of Compressor Fast Stop Using Cold Recycle System.

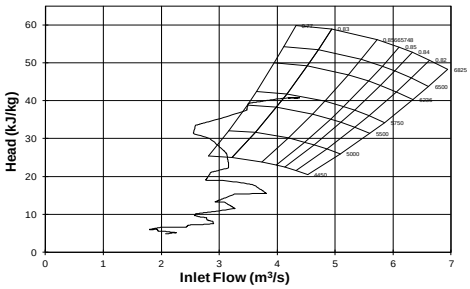

Figure 6: Field Measurements of Compressor Fast Stop Using both Cold and Hot Recycle Systems.

Table 1: Method I Example Calculation for Cold Recycle System Only and Initial Operating Point Shown in Fig. 4.

Flow Conditions:		
Suction Pressure	8202	kPa-a
Suction Temperature	283	K
Discharge Pressure	11352	kPa-a
Discharge Temperature	314	K
Average Compressibility	0.817	
Molecular weight	17.953	kg/kmol
Suction Density	76.560	kg/m3
Isentropic Exponent	1.482	
Isentropic Efficiency	0.8	
Mechanical Efficiency	0.96	
Gas Constant	463.098	J/kg.K
C_1	398.390	m/s
C_2	419.643	m/s
Suction Pipe Size		
Internal Diameter	0.737	m
X-Sectional Area (A_1)	0.426	m2
Discarge Pipe Size		
Internal Diameter	0.737	m
X-Sectional Area (A_2)	0.426	m2
Operating Point		
Q_o	4.363	m3/s
H_o	37072	J/kg
Q_{so}	3.482	m3/s
H_{so}	38863	J/kg
N_o	5500	RPM
ω	575.959	rad/s
Inertia	117	kg.m2
Results of Simple Approach :		
$(k-1)/k$	0.325	
ξ	329625.404	J/kg
S	1831.540	(J.s/kg.m^3)
dN_{max}/N_o	0.048	
dN_{max}	262.447	RPM
$d\omega$	27.483	rad/s
$\frac{\dot{m}_o H_o}{\eta_a \eta_m}$	16124.062	kW
$\delta tmax$	0.115	s
$\delta tmax$	115	ms

Table 2: Time for the Expansion and Compression Wave to Arrive at the Compressor Outlet and Inlet Respectively, from the Cold Recycle Valve.

Valve Pre-stroke delay	200	ms
Discharge Piping Length	42	m
Expansion Wave Arrival Time	100.09	ms
Combined Time	300.09	ms
Suction Piping Length	35	m
Pressure Wave Arrival Time	87.85	ms
Combined Time	287.85	ms

Table 3: Calculation for the Field Measurement Case of Fig. 5.

Flow Conditions:		
Suction Pressure	8202	kPa-a
Suction Temperature	283	K
Discharge Pressure	9340	kPa-a
Discharge Temperature	298	K
Average Compressibility	0.824	
Molecular weight	17.953	kg/kmol
Suction Density	75.951	kg/m3
Isentropic Exponent	1.482	
Isentropic Efficiency	0.8	
Mechanical Efficiency	0.96	
Gas Constant	463.098	J/kg.K
C_1	399.985	m/s
C_2	410.449	m/s
Suction Pipe Size		
Internal Diameter	0.737	m
X-Sectional Area (A_1)	0.426	m2
Discarge Pipe Size		
Internal Diameter	0.737	m
X-Sectional Area (A_2)	0.426	m2
Operating Point		
Q_o	3	m3/s
H_o	22500	J/kg
Q_{so}	2.8	m3/s
H_{so}	23500	J/kg
N_o	4000	RPM
ω	418.879	rad/s
Inertia	117	kg.m2
Results of Simple Approach :		
$(k-1)/k$	0.325	
ξ	332270.665	J/kg
S	1905.279	(J.s/kg.m^3)
dN_{max}/N_o	0.033	
dN_{max}	132.586	RPM
$d\omega$	13.884	rad/s
$\frac{\dot{m}_o H_o}{\eta_a \eta_m}$	6675.375	kW
$\delta tmax$	0.102	s
$\delta tmax$	102	ms

Table 4: Calculation for the Field Measurement Case of Fig. 6.

Flow Conditions:		
Suction Pressure	8202	kPa-a
Suction Temperature	283	K
Discharge Pressure	11450	kPa-a
Discharge Temperature	316	K
Average Compressibility	0.817	
Molecular weight	17.953	kg/kmol
Suction Density	76.560	kg/m3
Isentropic Exponent	1.482	
Isentropic Efficiency	0.8	
Mechanical Efficiency	0.96	
Gas Constant	463.098	J/kg.K
C_1	398.390	m/s
C_2	420.977	m/s
Suction Pipe Size		
Internal Diameter	0.737	m
X-Sectional Area (A_1)	0.426	m2
Discarge Pipe Size		
Internal Diameter	0.737	m
X-Sectional Area (A_2)	0.426	m2
Operating Point		
Q_o	4.39	m3/s
H_o	40160	J/kg
Q_{so}	3.62	m3/s
H_{so}	42900	J/kg
N_o	5700	RPM
ω	596.903	rad/s
Inertia	117	kg.m2
Results of Simple Approach :		
$(k-1)/k$	0.325	
ξ	329625.404	J/kg
S	1842.649	(J.s/kg.m^3)
dN_{max}/N_o	0.053	
dN_{max}	299.577	RPM
$d\omega$	31.372	rad/s
$\frac{\dot{m}_o H_o}{\eta_o \eta_m}$	17575.248	kW
$\delta tmax$	0.125	s
$\delta tmax$	125	ms

Table 5: Time for the Expansion and Compression Wave to Arrive at the Compressor Outlet and Inlet Respectively, from the Hot Recycle Valve.

Valve Pre-stroke delay	120	ms
Discharge Piping Length	5	m
Expansion Wave Arrival Time	11.88	ms
Combined Time	131.88	ms
Suction Piping Length	15	m
Pressure Wave Arrival Time	37.65	ms
Combined Time	157.65	ms

Method II: Inertia Number

Following numerous analyses conducted on different design philosophies of compression systems, and incorporating different types of centrifugal compressors, the decision to employ a short recycle system around the compressor unit to overcome the possibility of surging the unit during ESD operation lies in the balance between the following parameters:

- Effective compressor/driver rotor inertia defined at the compressor end, (I).
- Maximum compressor speed (N).
- The delay time before the recycle valve starts its opening stroke plus time taken for the first expansion wave or pressure wave to arrive at the compressor outlet or inlet, respectively, due to first crack-opening of the recycle valve (τ).
- The maximum fluid energy extracted from the compressor/driver power trains; which can be approximated by the product, where subscript (so) refers to conditions at the surge point and at the same maximum compressor speed.

A non-dimensional number was derived [18, 21] that includes all of the above independent parameters. This dimensionless number, herein referred to as the Inertia number (N_I), is defined as:

$$N_I = \frac{I N^2}{\dot{m}_{so} H_{so} \tau} \tag{12}$$

A threshold value of (N_I) was found from actual installations and dynamic analyses conducted on 24 industrial compression systems employing different compressor models and station design. This threshold value was found to be ~30, below which a shorter recycle system would definitely be needed to prevent the compressor unit from undergoing surge during ESD operation. When the Inertia number is greater than 100, a single recycle system (as shown in top of Figure 1) would be adequate. For an Inertia number (N_I) in the range of 30-100, detailed dynamic simulation on the station should be conducted (i.e. Method 3). Table 6 gives the various operating and design parameters for those 24 industrial compression systems analyzed and the respective Inertia number (N_I) based on a value of τ corresponding to the cold recycle system. Note that consistent SI units should be used to calculate (N_I). The comment column in Table 6 indicates whether the design incorporated a short (hot) recycle or not.

Station #8 shown in Table 6 is the example used in Method I above. It is shown that at 6,500 RPM, corresponding inertia

and $\dot{m}_{so} H_{so}$, the inertia number is 14.7, which is less than the threshold value of 30 discussed above. Therefore, it is pointing to the fact that the cold recycle system alone will not be adequate in protecting the compressor unit from surging during an ESD or fast stop.

Table 6: Inertia Numbers of 24 Industrial Gas Compressor Stations and Comparison with the Present Compressor Station.

Station	I (kg.m^2)	N (RPM)	Flow (kg/s)	Hso (J/kg)	τ (ms)	No of Stages	Cooler	Inertia Number	Comment
1	36.1	6800	250	28000	200	1	No	13.1	Delay in Fuel Gas by 100 ms
2	33.7	8856	143	80600	200	2	Yes	12.6	Hot & Cold Recycle Installed
3	32.2	7780	125	64500	200	2	Yes	13.3	Hot & Cold Recycle Installed
4	56.5	6500	180	52000	200	2	Yes	14.0	Hot & Cold Recycle Installed
5	41.5	6671	150	40000	200	2	Yes	16.9	Hot & Cold Recycle Installed
6	243.6	6100	299	68772	200	2	Yes	24.2	Hot & Cold Recycle Installed
7	259.6	4250	380	26220	200	1	Yes	25.8	Hot & Cold Recycle Installed
8	117.0	6500	244	52625	288	2	Yes	14.7	Hot & Cold Recycle Installed
9	102.5	6000	35	160000	215	6	Yes	33.6	Hot & Cold Recycle Installed
10	113.5	6825	420	31000	588	1	Yes	7.6	Hot & Cold Recycle Installed
11	3.9	11967	3	117000	337	4	Yes	54.0	Hot & Cold Recycle Installed
12	6.1	11970	9	124386	324	4	Yes	27.6	Hot & Cold Recycle Installed
13	104.8	7850	51	160612	368	5	Yes	23.4	Hot & Cold Recycle Installed
14	94.3	8311	50	152825	368	6	Yes	25.3	Hot & Cold Recycle Installed
15	0.2	20000	20	32000	185	1	No	6.5	Hot Recycle
16	128.6	5194	480	32000	200	1	No	12.4	Hot Recycle
17	870.0	5775	350	39000	200	2	Yes	116.6	Only Cold Recycle
18	1.885	14000	5.00	154000	260.29	6	Yes	20.2	Hot & Cold Recycle Installed
19	29.86	8000	104.9	58400	200	2	Yes	17.1	Hot & Cold Recycle Installed
20	29.86	8000	58	59200	200	2	Yes	30.5	Hot & Cold Recycle Installed
21	24.6	9053	154	52130	190	2	Yes	14.5	Hot & Cold Recycle Installed
22	24.6	9500	155	56947.72	200	2	Yes	13.8	Hot & Cold Recycle Installed
23	147.3	5000	550	36400	200	2	Yes	10.1	Hot & Cold Recycle Installed
24	80.9	6400	550	25471	200	1	Yes	13.0	Hot & Cold Recycle Installed

Method III: Full Dynamic Simulations

In a full numerical dynamic simulation of such compression systems, it is important to include the temporal-spatial dependence terms in all three governing equations for the gas flow in each piping element. In many of the commercial codes, only the time gradients are considered in the dynamic simulations, which amounts to describing the dynamics of the system using Ordinary Differential Equations (ODEs) that are much less rigorous than the Partial Differential Equations (PDEs). This is referred to as the "lumped parameter" method, which gives a solution that is a reasonable approximation of the distributed model solution. However, the lumped parameter approach is not adequate for dealing with compression dynamics involving recycle systems and phenomena of compressors going into, and out of, surge. The spatial gradients along the length of the pipe segments are crucial, as was determined from the previously discussed "*Method I*". The spatial gradients describe the time required for perturbations in pressure, flow, and temperature to propagate from one point in the system to another.

The methodology in the dynamic simulations conducted here retains all terms in the one-dimensional governing PDEs described below [18, 21 through 28]:

Continuity:

$$\frac{\partial \rho}{\partial t} + \rho \frac{\partial u}{\partial x} + u \frac{\partial \rho}{\partial x} = 0 \tag{13}$$

Momentum:

$$\rho \frac{\partial u}{\partial t} + \rho u \frac{\partial u}{\partial x} + \frac{\partial P}{\partial x} - \beta = 0 \tag{14}$$

Energy:

$$\frac{\partial P}{\partial t} + u \frac{\partial P}{\partial x} - c^2 \left(\frac{\partial \rho}{\partial t} + u \frac{\partial \rho}{\partial x} \right) - E = 0 \tag{15}$$

where;

$$\beta = -\left[\frac{f_{DW}}{2D} \rho u |u| + \rho g \sin(\theta) \right] \tag{16}$$

$$E = \phi \left(q_h - u \beta \right) \tag{17}$$

$$\phi = \frac{\rho}{T} \left(\frac{\partial T}{\partial \rho} \right)_s = \frac{1}{\rho C_v} \left(\frac{\partial P}{\partial T} \right)_v \tag{18}$$

$$q_h = \frac{4U_h}{D} \left(T_a - T \right) \tag{19}$$

Note that the effects of both pipe wall friction and heat transfer with the surroundings are accounted for in the conservation of energy via the parameter, *E*, in Eq. (17). Using the method of characteristics, the above hyperbolic partial differential equations are transformed into ordinary differential equations, which lead to a set of algebraic compatibility equations along two characteristic lines and a particle path line [22]. These compatibility equations, together with the respective characteristic lines are integrated in the time-space domain. In the derivation of the finite-difference compatibility equations, the real gas assumption is introduced and GERG-2008 [29] equation of state is employed to specify the relation between the gas density, temperature, pressure and enthalpy, as well as to determine the physical and thermodynamic properties at each node in the system.

Similar governing equations describing the transient flows through physical components in the system are also formulated and combined with Eq. (13-15). These elements are throttle or pressure loss elements, combining and dividing tees, reducers or expanders, capacitance (plenum, volume,

vessels), choked and un-choked valves, aerial coolers with a set duty or a set outlet temperature, etc. A full account of the governing equations for these elements is given in [23]. Throttle elements and capacitance elements are modeled based on quasi-steady state equations describing pressure changes as well as energy and mass balances across the element. These equations, when combined with the three compatibility equations for the pipes connected upstream and downstream of the element, are solved simultaneously to give the unknown variables on both sides of the element at each time step. Different formulations of the equations are used to account for reversed flow situations.

The compressor itself is assumed to respond to any perturbation in a quasi-steady manner following its full characteristic curve, including that to the left of the surge limit [2,3,18,19]. At a given flow to the left of the surge limit, however, the actual head may differ from the steady state characteristics, which is the consequence of the compressor going into surge. A physically realistic and commonly used representation of this characteristic is that of a simple cubic given by the following equation [15,16]:

$$H_a = H_Z + \gamma\left[1 + 1.5\left(\frac{2Q_a}{Q_s} - 1\right) - 0.5\left(\frac{2Q_a}{Q_s} - 1\right)^3\right] \quad (20)$$

Where:

- Q_a - compressor actual inlet flow
- H_a - compressor adiabatic head at any given inlet flow (Q_a)
- H_z - compressor adiabatic head at zero flow = $\alpha\sum_1^n U_i^2$
- γ - parameter = 0.5 (H_s-H_o)
- α - zero flow head coefficient (equal to 1.0 for loss free impeller, and approx. equal to 0.4-0.6to account for losses)
- U_i - rotational tip velocity of impeller (i)
- H_s - compressor head at surge point at the current running speed
- Q_s - compressor actual inlet flow at surge point at the same speed
- D_o - impeller outer (tip) diameter
- D_i - impeller average inlet diameter

Compressor/driver dynamics are governed by Eq. (1); relating the driver power to the gas power and the inertias of both driver and compressor. It should be noted that the driver and compressor inertias should also include the inertia of the elements of the gearbox and couplings connected to either side, respectively. Additionally, in the case of a two-shaft gas turbine driver, the applicable driver inertia in Eq. (1) above is only the power turbine (i.e. the driver rotor) and coupling inertias and is not inclusive of the gas generator inertia.

Finally, a compression system consists of most of the elements described above, whether it is a pipe element, a connecting element or boundary condition. These constitute sets of highly non-linear equations, which must be solved simultaneously to determine the unknowns (pressure, mass flow rate, and temperature). Each set of equations requires solution at each Δx location along each pipe element at each Δt time step. To achieve numerical stability, the Courant stability condition [30] is applied which stipulates that:

$$\Delta t \le \frac{\Delta x}{C + v} \quad (21)$$

The Newton-Raphson method for the solution of non-linear equations is used because of its convergence speed and efficiency. The method is iterative in nature and solves all equations simultaneously. The starting point for a variable at a given time step is the value obtained as a solution from the previous time step. With small time steps (required by the stability condition), parameter changes longer than this time step will be captured and therefore transients occurring over several time steps will certainly be accounted for. Variables calculated at a given time step represent a good starting point for the next time step calculation. The iteration process within each time step is continued until the desired solution tolerance is achieved. Generally, the required calculation accuracy is obtained in under ten iterations at each time step.

Finally, at each time step, a set of Mixed Algebraic and ODE's equations (constituting a MAD set) which describe the governing equations of the connected control system. These equations are solved simultaneously at each time step in a different solver routine. The output from the control system solver is then fed to the gas dynamic solver described above and act as set points, constraints or boundary conditions.

CASE STUDY

This case study is an example of a compression facility that employs 8 compressor units in total; Units 1 through 5 are slow speed integral compressors and Units 6 through 8 are gas turbine driven centrifugal compressors. Unit 8 is the latest addition to the station and operates in parallel with Units 6 and 7. The addition of Unit 8 meant a number of station layout modifications were necessary. These included: re-wheeling of Units 6 and 7 (i.e., change the compressor impellers); addition

of gas after cooling; and relocating the anti-surge valves downstream of the coolers to allow for both hot (fast stop) and cold recycle (anti-surge) capabilities. Due to the addition of equipment and significant reconfiguration of station piping and valves, a dynamic surge analysis on Units 6, 7, and 8 was required to determine whether the existing anti-surge and fast stop valves were adequately sized and whether the anti-surge valves could be relocated downstream of the gas coolers. A fast stop recycle system was also considered for the newly added Unit 8, which also needed to be adequately sized.

Units 6 and 7 are similar OEM and model number compressors driven by gas turbines, while Unit 8 is a different OEM compressor also driven by a gas turbine. The combined rotor inertia of Unit 6 compressor/power turbine assembly (which is the same for the other two Units) is 24.6 kg/m^2. The compressor performance characteristics (wheel maps) including the full characteristics to the left of the surge line are given in Fig. 8, respectively. The initial steady state operating points on the three Units are indicated on the respective wheel maps, and are also given in Table 7. The mixture composition of the gas flowing through the station is given in Table 8. Finally, the selected recycle valves (hot and cold) for the three Units are given in Table 9 along with the estimated pre-stroke delay and full-stroke opening time, respectively. Of notice is that the hot valve capacity is larger for Unit 8 than that for Units 6 and 7 due to the relatively large volume of gas trapped between the hot recycle and check valves on the discharge side of Unit 8 (approx. 13.7 m^3) vs. that on the discharge side of either of Units 6 or 7 (3.3 m^3 and 5.7 m^3, respectively).

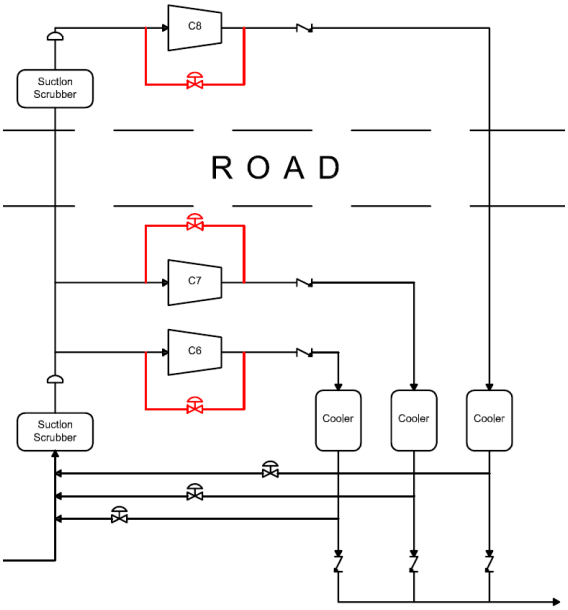

Figure 7: Schematic of the Case Study Involving Three Compressor Units Configured in Parallel Operation.

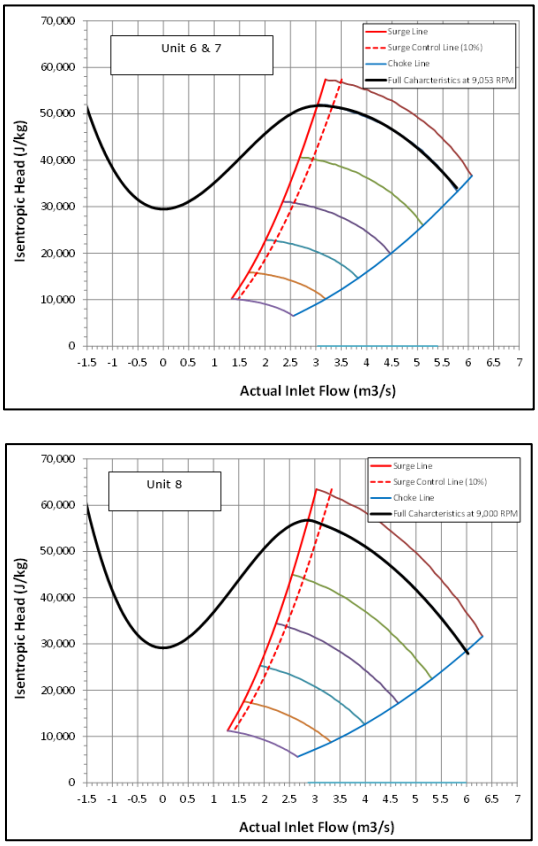

Figure 8: Compressor Performance Characteristics of Units 6 and 7 (top) and Unit 8 (bottom) Showing Full Characteristics at One Speed and the Respective Initial Steady State Operating Point.

Table 7: Initial Steady-State Operating Points of Units 6, 7, and 8.

		Parallel		
		Unit 6	**Unit 7**	**Unit 8**
Suction Pressure	Ps (MPa-a)	5.598	5.597	5.597
Discharge Pressure	Pd (MPa-a)	8.168	8.168	8.169
Suction Temperature	Ts (°C)	10.0	10.0	10.0
Discharge Temperature	Td (°C)	48.9	48.9	47.9
Compressor Mass Flow Rate	mC (kg/s)	165.6	165.3	181.4
Compressor Actual Inlet Flow Rate	Qa (m3/s)	3.72	3.71	4.07
Compressor Isentropic Head	H (kJ/kg)	50.8	50.8	50.8
Compressor Speed	RPM	9,062	9,062	9,020

Table 8: Gas Mixture Composition.

	Mole %
METHANE	97.317
ETHANE	2.332
PROPANE	0.095
i-BUTANE	0.002
n-BUTANE	0.006
NITROGEN	0.203
CARBON DIOXIDE	0.045
Total	100.00

Table 9: Hot and Cold Recycle Valve Sizes, Trim Types and Capacities for the Three Units.

	Function	Location	Size	Cg	Trim	Pre-Stroke Delay (ms)	Full Stroke Time (ms)
Unit 6	Fast Stop Valve	Hot Recycle	8"	37,000	Quick Open	100	400
	Anti-Surge Valve	Cold Recycle	10"	44,000	Eq %	100	660
Unit 7	Fast Stop Valve	Hot Recycle	8"	37,000	Queck Open	100	400
	Anti-Surge Valve	Cold Recycle	10"	44,000	Eq %	100	660
Unit 8	Fast Stop Valve	Hot Recycle	8"	48,000	Linear	100	400
	Anti-Surge Valve	Cold Recycle	10"	48,000	Eq %	100	660

The corresponding inertia numbers for all three Units were first calculated based on the aforementioned information with respect to each Unit. The calculation results are shown in Table 10, which indicate that all three Units have inertia numbers much lower than the threshold value of 30 discussed earlier.

Table 10: Calculated Inertia Numbers for Units 6, 7, and 8 (*cf*. Eq. 12).

	Units 6&7	Unit 8
I (kg.m2)	24.6	24.6
N (RPM)	9053	9500
Flow (kg/s)	154	155
Hso (J/kg)	52130	56947.721
τ (μs)	190	200
No of Stages	2	2
Cooler	Yes	Yes
Inertia Number	**14.49**	**13.79**

As a result, dynamic simulations were conducted to assess the adequacy of the selected recycle valves for preventing the Units form undergoing surge if all Units are subjected to an ESD or Fast Stop procedure. The results are shown in Fig. 9, which indicate a normal pattern of all units winding down along an H-Q path to the right of the respective surge lines. This is a good indication of the adequacy of the size, trim type and opening time characteristics of the selected valves. Note that, in the event of an ESD or Fast Stop, both hot and cold recycle valves around each Unit would open according to the estimated opening time indicated in Table 9.

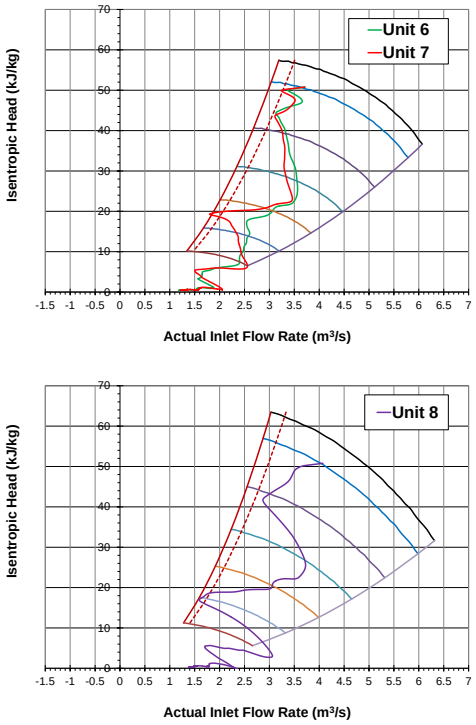

Figure 9: Head-Flow Trajectories of the Three Units on the Respective Wheel Maps Following ESD or Fast Stop of All Three Units Simultaneously.

The question that arises is what happens if one Unit is subjected to ESD or fast stop, while the other two Units are kept running. Results of dynamic simulation of an ESD or fast stop operation of either Unit 6 or Unit 7, while keeping the other two Units running are shown in Fig. 10 (in this case, Unit 6 is subjected to ESD). Similar results were obtained if Unit 7 is subjected to ESD, since both Units 6 and 7 are alike. The results show that the two other Units that are kept running, were subjected to small disturbances but stayed on the same speed and discharge pressure control without being forced to go to surge.

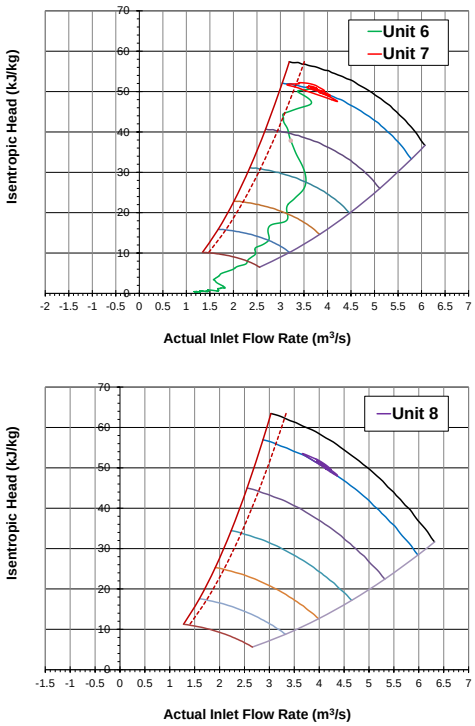

Figure 10: Head-Flow Trajectories of the Three Units on the Respective Wheel Maps Following ESD or Fast Stop of Only Unit 6, While Units 7 and 8 Continue to Run.

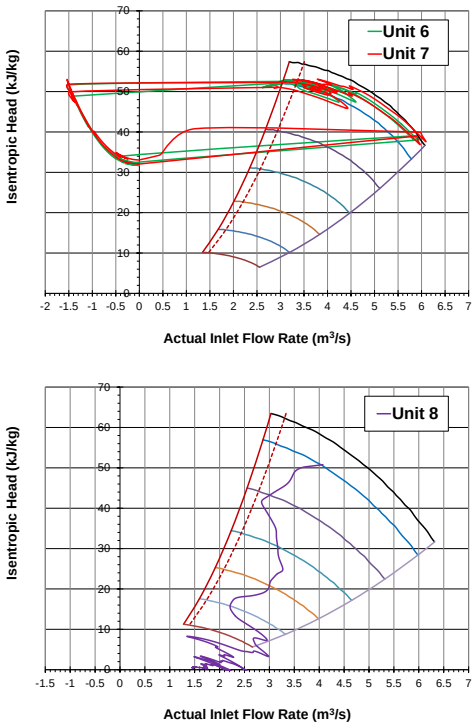

Figure 11: Head-Flow Trajectories of the Three Units on the Respective Wheel Maps Following ESD or Fast Stop of Only Unit 8, While Units 6 and 7 Continue to Run.

However, the situation is different when Unit 8 is subjected to ESD or fast stop while the other two identical ones, i.e., Units 6 and 7, are kept running. The results of the dynamic simulation of this case are shown in Fig. 11, which shows that Unit 8 wound down surge free while both Units 6 and 7 have undergone two surge cycles, and each cycle lasts approximately 0.8-0.9 s as shown in Fig. 12. These two surge cycles may be acceptable since they are only two, and that two respective compressors recover back to normal operation following these two quick surge cycles, albeit still at the respective high heads.

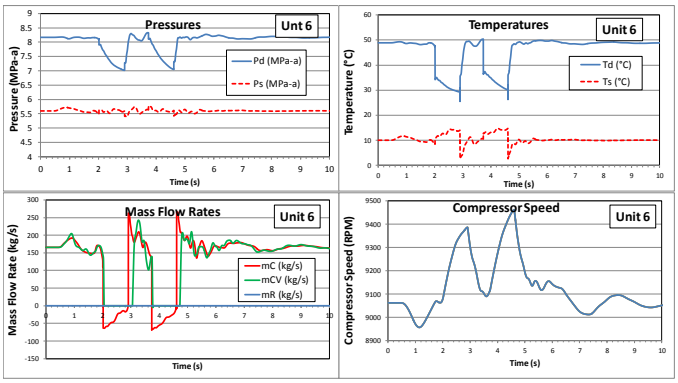

Figure 12: Pressure-, Flow-, Temperature- and Speed-Time Profiles of the Running Unit 6 Following ESD or Fast Stop of Unit 8, While Units 6 and 7 Continue to Run.

Dynamic Simulations Based on Newly Acquired Recycle Valves

Following the above analysis, a recommendation was made to replace the current recycle valves for Units 6 and 7, and, of course, acquire hot and cold recycle valves for the newly added Unit 8. All six acquired valves have flow-opening characteristics (trim characteristics) depicted in Fig. 13. These valves are full-bore ball type valve and hence their opening characteristics are akin to that of a modified equal percentage type trim. Additionally, all valves were shop-tested to determine the exact pre-stroke delay and full stroke opening time. Figure 14 shows an example of these tests for Unit 6 hot and cold recycle valves, respectively. Note that these valves reach 90% open in a linear fashion, while the remaining 10% takes much longer time. Therefore, in all of the dynamic simulations to follow, the respective capacities of these valves corresponding to their 90% open were taken as their respective capacity/time limits for the purpose of the dynamic simulations. The other four valves (for Units 7 and 8) showed similar trends and all six valves characteristics are given in Table 11.

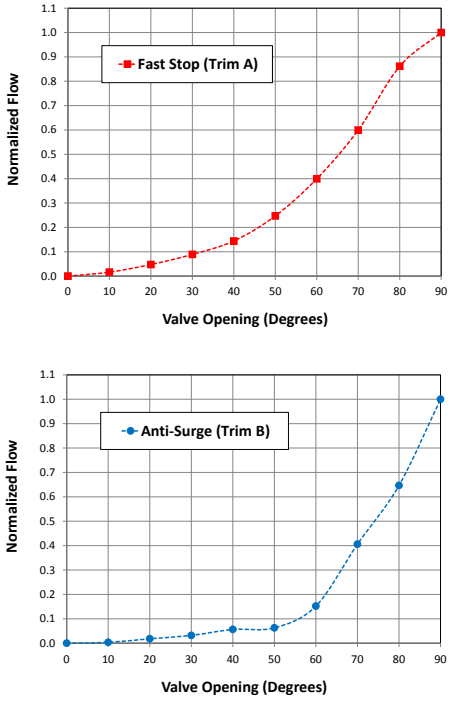

Figure 13: Hot (Fast Stop) and Cold (Anti-Surge) Valve Flow Characteristics for the Newly Acquired Valves.

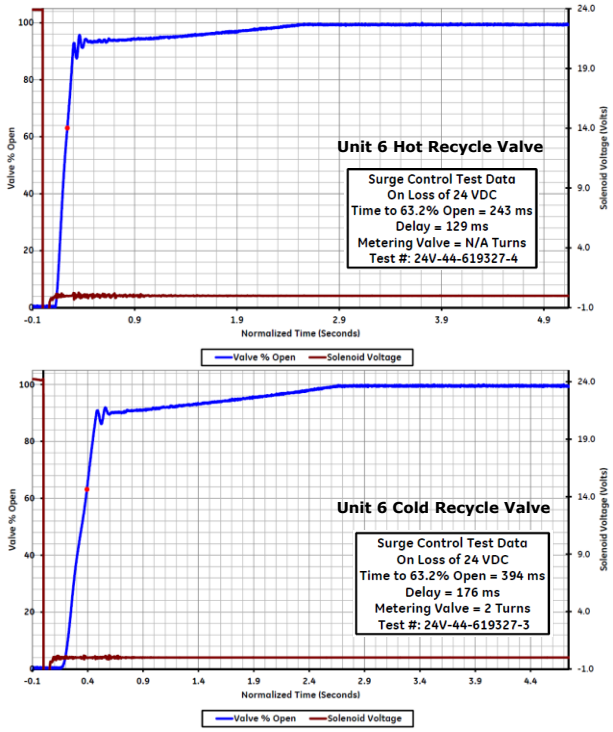

Figure 14: Shop Test Results of Unit 6 Hot and Cold Recycle Valves.

Table 11: Hot and Cold Recycle Valve Characteristics of the Six New Valves Purchased for Three Compressor Units.

	Unit 6		Unit 7		Unit 8	
	Hot Reccyle	Cold Recycle	Hot Reccyle	Cold Recycle	Hot Reccyle	Cold Recycle
Nominal Size	8"	10"	10"	10"	8"	10"
Tag #	FV-51510	FV-0660	FV-0761	FV-0760	XV-0861	FV-0860
Model	FPBV-S	QTCV-T2	FPBV-S	QTCV-T2	FPBV-S	QTCV-T2
Pre-Stroke Delay (ms)	129	176	127	176	115	203
Stroke to 90% open (ms	170	312	240	312	187	230
Cv	5,250	3,399	8,500	3,399	5,250	3,399
Characteristics	Trim A	Trim B	Trim A	Trim B	Trim A	Trim B

The foregoing dynamic simulation models were repeated using the now exact valve flow characteristics (Fig. 13), pre-stroke and stroke times (Table 11). Four simulations were conducted for the following ESD cases:

a) ESD of all three units (6, 7, and 8) at the same time.
b) ESD of only Unit 6, while Units 7 and 8 continue to run.
c) ESD of only Unit 7, while Units 6 and 8 continue to run.
d) ESD of only Unit 8, while Units 6 and 7 continue to run.

The results of these simulations are shown in figures 15 through 19. Figure 15 shows the results of the first dynamic simulation of an ESD applied to all three Units (6, 7 and 8) at the same time. It is evident that all three Units wind down in a normal manner and that none has undergone any surge cycle. This indicates that the new valves are adequate to protect all three Units from surging. Note also that the wind-down head-flow paths for Units 6 and 7 exceed the choke (stone-wall) limit of the compressor. This is not to be alarmed about, since in reality the compressor will limit the flow along its choke limit curve (which is not necessarily the one shown in the Figure). As long as the H-Q path during compressor wind down is away from the respective surge limit, the compressor is safe and protected from surging during ESD.

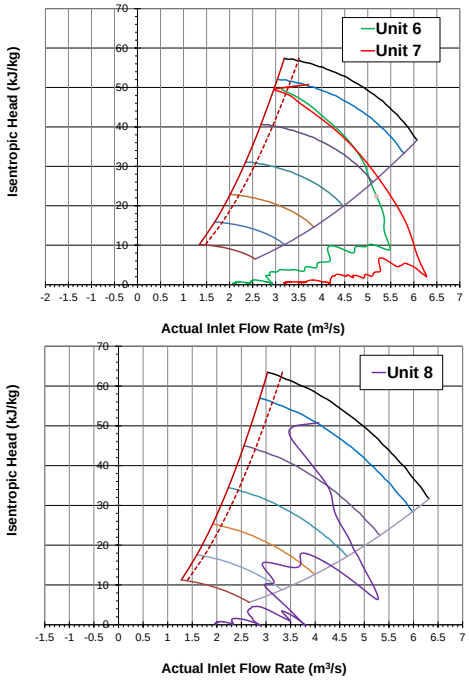

Figure 15: Head-Flow Trajectories of the Three Units on the Respective Wheel Maps Following ESD or Fast Stop of All Three Units at the Same Time.

The results of the second simulation involving ESD of Unit 6 only, while the other two Units continue to run, showed that Unit 6 winds down free-of surge. However, the adjacent Unit 7 that continued to run experienced several surge cycles as shown in Fig. 16. The duration of each surge cycle is shown to be approximately 1.5-1.8 s. Unit 8, being farther away did not undergo any surge cycle in this case. Similar trends are observed in the third simulation case when Unit 7 was subjected to ESD while the other two units (6 and 8) continue to run. In this case, Unit 6 went into several surge cycles as depicted in the results shown in Fig. 17. Again, Unit 8 did not go into surge in this case.

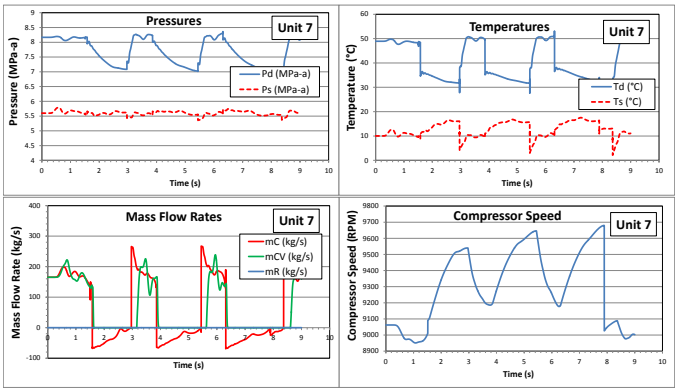

Figure 16: Pressure-, Flow-, Temperature- and Speed-Time Profiles of the Running Unit 7 Following ESD or Fast Stop of Unit 6, While Units 7 and 8 Continue to Run.

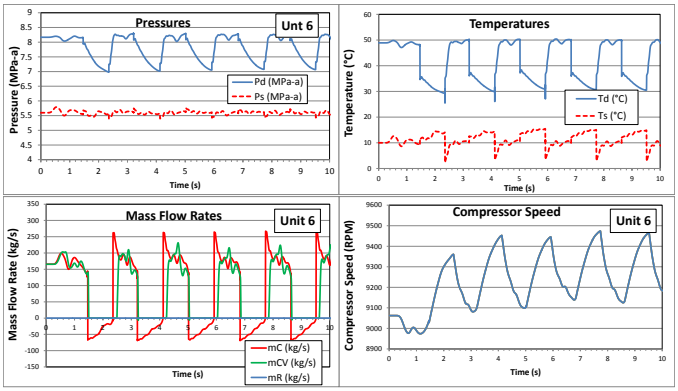

Figure 17: Pressure-, Flow-, Temperature- and Speed-Time Profiles of the Running Unit 6 Following ESD or Fast Stop of Unit 7, While Units 6 and 8 Continue to Run.

The last simulation involved ESD of Unit 8 while Units 6 and 7 continue to run. The results are shown in Figs. 18 and 19 indicating that both Units 6 and 7 experienced several surge cycles, while Unit 8 is winding down normally without any sign of surging.

From the foregoing four simulation results, it is evident that valve sizes, capacities, flow characteristics, and opening time of all the newly acquired recycle valves are adequate in protecting their respective Units from surging during ESD. However, surging of other running Units when an adjacent Unit is fast-stopped or ESD is rather due to the dynamic disturbances in flow and pressure that brings about instabilities to the other operating (on line) Units, particularly when the other Units were operating close to their respective

surge lines. In order to alleviate this problem, one option is to implement a control strategy such that if any one of the three units is subject to ESD or fast stop, the other two Units should automatically be fast stopped to protect them from surging. Clearly, this is not desirable both from operational perspectives, as well as from reliability and commercial obligation of meeting gas volume delivery to customers.

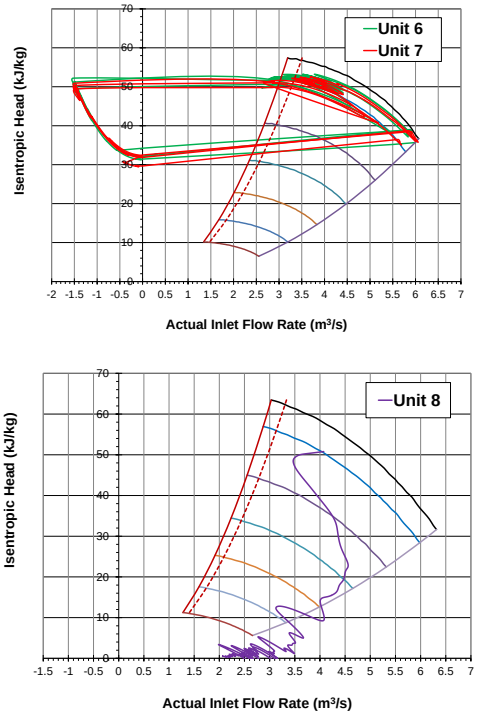

Figure 18: Head-Flow Trajectories of the Three Units on the Respective Wheel Maps Following ESD or Fast Stop of Only Unit 8, While Units 6 and 7 Continue to Run.

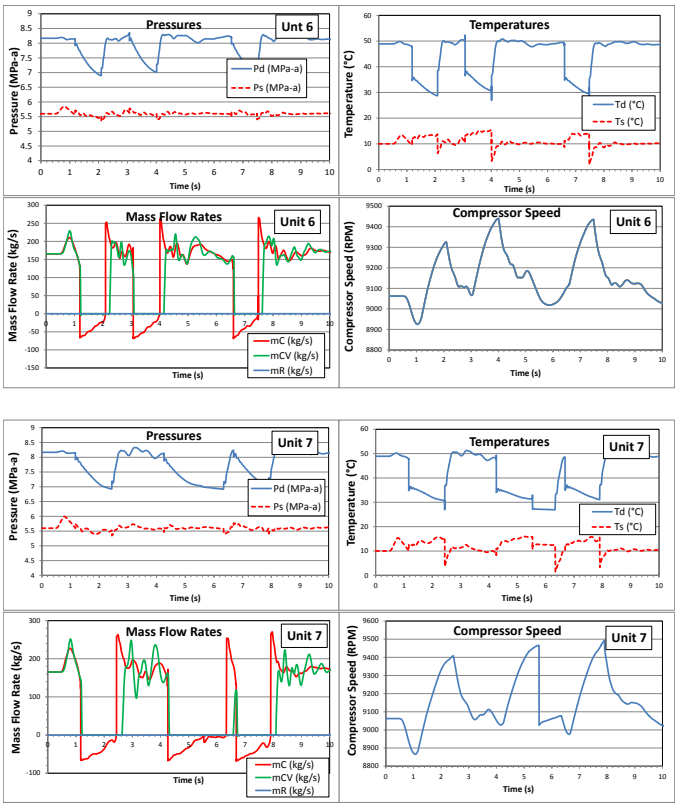

Figure 19: Pressure-, Flow-, Temperature- and Speed-Time Profiles of the Running Units 6 and 7 Following ESD or Fast Stop of Unit 8.

Therefore, the main cause for a Unit surging when the adjacent Unit is fast-stopped is investigated further in an attempt to identify the symptoms and develop a correction to circumvent it. A closer look at the results of Fig. 16 showing Unit 7 surging when Unit 6 is fast-stopped reveals that the precursor to the first surge cycle is a pronounced overshoot of the mass flow through Unit 7 resulting from the 'dump' of excessive flow from the oversized hot and cold recycle valves around Unit 6. The overshoot in flow translates to lower head since the speed of the compressor cannot react within such a relatively short time duration. Subsequent to this overshoot, and as the power turbine is delivering the same power (no time for the fuel gas controller to react), an undershoot of flow is rapidly developed to bring the flow back to the operating point. An overshoot followed by the undershot vividly depicted in Fig. 20, following which, the compressor went into the first surge cycle due to the severe dynamics of the gas flow.

So, in order to circumvent this, the apparent overshoot in the flow needs to be dampened. This can be achieved by moderating the excessive flow 'dump' from the recycle systems around Unit 6. One concept is to set the anti-surge valve (cold recycle valve) to a normal stop mode, in which case it would close in 1000 ms rather than 312 ms (*cf.* Table 11). A dynamic simulation was then conducted to emulate this approach and the results are shown in Fig. 21. It is shown that the overshoot was dampened on Unit 7, and resulted in preventing the compressor from surging when Unit 6 is fast-stopped. The same protocol can also be applied to Unit 7 anti-surge valve opening when Unit 7 is subjected to ESD or fast stop.

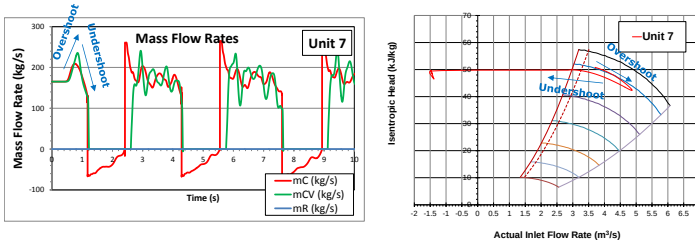

Figure 20: Evidence of Overshoot Followed by Undershoot of Unit 7 Flow When Unit 6 is Fast-stopped.

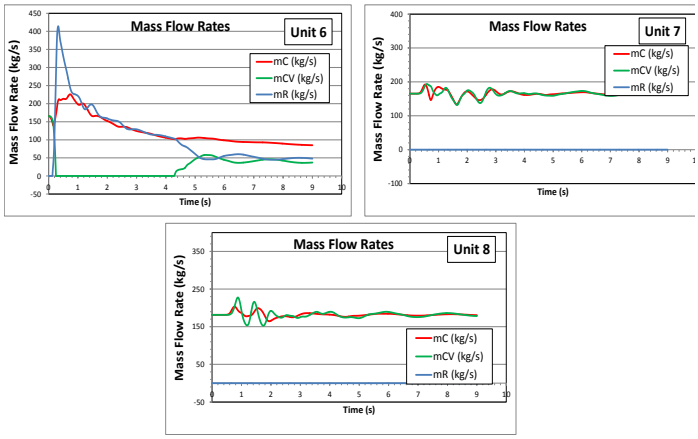

Figure 21: Results of Dynamic Simulation Showing Surge-Free Unit 7 When Unit 6 Is Fast-Stopped If Its Cold Recycle Valve Opening Time Is Set to Normal Shutdown Protocol.

When the above protocol is applied to Unit 8 when it is fast-stopped, results from dynamic simulation showed that the problem of both Units 6 and 7 surging persists, even if Unit 8 anti-surge valve was not opened at all. This directed attention to Unit 8 fast stop (hot recycle) valve. A dynamic simulation showed that if this valve was smaller (e.g., Cv=1250) but has a quick-open trim and fully opens even in 500 s, Units 6 and 7 will not surge if Unit 7 is fast stopped. This led to comparing the newly acquired valve (larger capacity of Cv=5250 but opens in very short time, i.e. 265 ms) to the originally selected valve of Cv=1250 with a quick-open trim and fully opens in 500 ms. This comparison is shown in Fig. 22. A hint could be immediately drawn from Fig. 22 in that, for the newly acquired large capacity valve to match that of the originally selected valve, it could be set to open only to 53 degrees (recall that it is a ball valve), at the same opening rate as is set by its actuator. This can be achieved by limiting its stoke to this desired opening angle by implementing a stop to its maximum opening position. In this case it will open to the desired 53 degrees in approximately 150 ms as shown in Fig. 22.

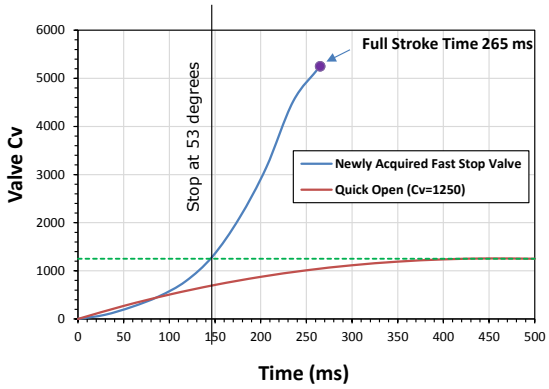

Figure 22: Comparison Between the Opening and Flow Characteristics of the Newly Acquired Ball Valve vs. the Originally Selected Quick-Open Trive Valve for Unit 8 Fast Stop Valve.

The above concept was then tested via a dynamic simulation with two changes to Unit 8 recycle valves. The first is either to open the anti-surge valve at a normal compressor shutdown opening rate (e.g. over 1000 ms or longer), or not to open it at all when Unit 8 is fast-stopped. The second, which is to limit the opening of the fast stop (hot recycle) valve to 53 degrees at the same dump rate allowed by the actuator-solenoid set. The results of this simulation are shown in Fig. 23. It is shown that Unit 8 winds down normally when subjected to ESD or Fast Stop, while both Units 6 and 7 continue to run without the risk of undergoing surge.

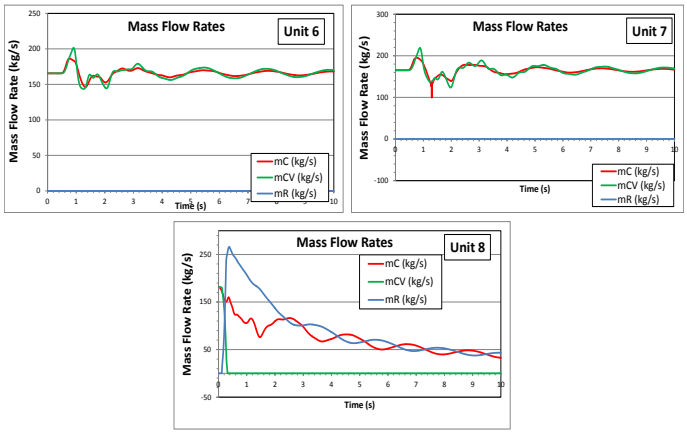

Figure 23: Results of Dynamic Simulation Showing Surge-Free Units 6 and 7 When Unit 8 is Fast-Stopped if its Hot Recycle Valve is Limited to Open to 53 degrees.

DISCUSSION

This paper can be useful to those in the industry not intimately familiar with surge design or analysis methods. Examples include Project Managers with backgrounds other than rotating equipment, operations personnel, and other less technical positions. First, it describes what surge is, typical surge behavior, and why it is important to design a robust surge is control system. Additionally, this paper describes how surge can damage centrifugal compressors if a surge control system is inadequately designed. This is important as compressor repair and/or replacement costs can be exceedingly high as a result of lost downtime (lost revenue), equipment, and premium-time labor costs.

The methods given herein provide consideration to the spatial aspects of a particular system design that are not accounted for using lumped volume parameter methods. Each compressor installation has its own compressor characteristics (often called wheel maps), piping design, and flow conditions, and therefore cannot be generalized by ignoring the spatial considerations (i.e., lengths of pipe). Doing the latter can lead to a false sense of security in the surge protection design for a given system.

Methods 1 and 2 provide tools to compressor system designers to 1) better determine whether the system in question requires a hot recycle system, 2) if the recycle systems as designed will be adequate in preventing surge, and 3) when a detailed dynamic simulation (Method 3) of the system is required. The tools can also be useful to end users, and EPCs desiring to check the adequacy of systems proposed by vendors.

In some cases surge cannot be avoided, and going into one surge cycle may be tolerated. Method 3 provides the opportunity to determine the severity of a particular surge event. The simulation determines how deep a particular surge case will be, for how long, and how many cycles the unit will go in and out of surge during one fast stop event, providing the information needed to make a decision on whether to except the surge or not.

Method 3 also gives the opportunity to analyze how complicated systems with multiple compressors will behave and interact together. Simulations of this nature can help reduce the overall facility risk by foreseeing upset conditions as shown in the previous case, thus increasing the reliability achieved in a particular installation.

In an effort to demonstrate some complexities that can arise in the real world, a case study of a major gas pipeline operator compressor station is provided. The scope of this compressor station expansion project included converting the station to accommodate reverse flow capability, addition of after gas coolers to units 6 and 7, and the addition of unit 8 with gas after cooling. As part of the addition of gas after cooling for units 6 and 7, significant piping changes were made to the suction and discharge headers to allow for a hot and cold recycle, as discussed previously. As such, the operating company engineers grew increasingly concerned that the surge control systems for units 6 and 7 would not be adequate, given significant piping additions leading to increased volume, relocation of surge valves, and the addition of a new centrifugal compressor unit. This concern grew out of the fact that the compressor OEM typically uses a “lumped parameter” analysis method to provide recommendations for surge control design. On typical projects, lumped parameter results are provided to the EPC for final piping design and valve procurement, installation, and operation.

Given the complexities of this project, the operator felt it would be prudent to utilize Method III as described herein instead of the lumped parameter method. The analysis was completed without impact to the overall project schedule and was coordinated successfully with the EPC. The Method III analysis results and recommendations were issued to the operator prior to major procurement activities, which allowed for procurement of the surge control valves. There are important procurement considerations which warrant discussion.

The hot recycle valve purpose involves unloading the compressor in the fastest possible manner. Numerous simulations have shown that systems can be very sensitive to the valve opening characteristics in terms of whether a

compressor will reach surge or not. Figure 24 shows typical valve opening characteristics (trims). As can be seen from Fig. 24, 50% opening of a quick open valve will admit 80% of the maximum flow, while an "equal percentage" (ball design) valve at the same opening would only admit 20% of the maximum flow. A hot recycle application is best served with a "quick opening" valve, usually achieved with a globe type valve design.

The problem that can arise with procurement is a communication one. Recycle valve manufacturers may claim that their valve is a "quick open" style, and they would be right, in that their valve opens within a couple of hundreds of milliseconds. But a quick opening (time-wise) of an equal percentage (trim-wise) valve would still be inferior to a slower opening (time-wise) "quick opening trim" valve in this application. For this obvious confusion point, the authors recommend specifying a globe type valve for hot recycle applications.

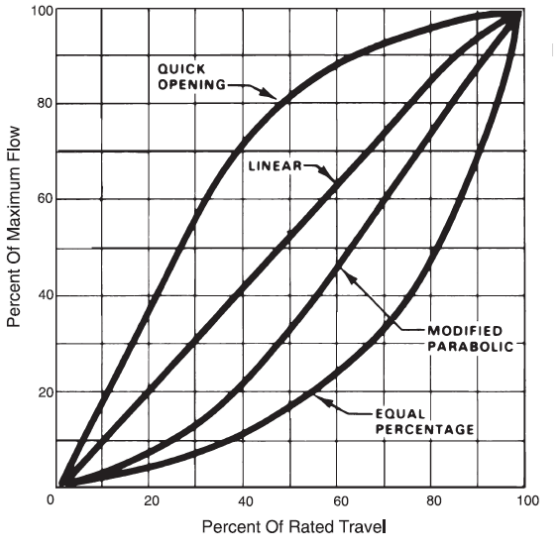

Figure 24: Valve Opening Characteristics

In terms of this project, the "quick open" valve recommendation resulted in the procurement of quickly opening equal percentage style valves, which provided a slightly inferior system than if the globe style valve had been ordered. Luckily in this case, a solution was found to still use the newly acquired valves by making thoughtful adjustment of their respective opening protocol based on extensive dynamic simulations of different ideas. This allowed any one unit to be fast-stopped or ESD while the other two continue to run.

CONCLUDING REMARKS

The old belief that "a single combined surge/recycle line is acceptable and is commonly used in the industry in the design of compressor stations" should be re-examined vigilantly. This paper presents three methodologies to assess the adequacy of such a single combined surge/recycle system to protect the compressor from undergoing deep surge during ESD.

It is also important to recognize the influence of salient parameters that play a key role in the dynamics of the recycle systems in compressor stations for all intended purposes and functions, namely: startup, part loads, surge control, and surge protection following ESD or fast-stop. These very key parameters are:

1. Compressor/power turbine rotor inertia;
2. Compressor pressure ratio (i.e., compressor adiabatic head);
3. Volumetric capacitance of recycle system;
4. Recycle system response time (i.e., recycle valve pre-stroke delay, stroke time, time of arrival of expansion and pressure wave from the recycle valve to the compressor outlet and inlet, respectively);
5. Compressor performance characteristics; and
6. Flow capacity of the recycle system.

The designer should always consider all of the above parameters with the aid of the methodologies presented in this paper. These methodologies with the aid of dynamic simulations should facilitate the right decision in designing an adequate recycle system for the benefit of equipment integrity, performance and safety.

ACKNOWLDEGEMENTS

The authors wish to sincerely thank Russ Barss for his foresight in promoting attention to the use of the right analysis tool to designing surge control systems.

The support, help, and ideas received from Jackie Walters, Hilmar Bleckmann, and Jeff Vea to prepare this paper are greatly appreciated. Special thanks to Mark Sandberg for his efforts during the preparation of the paper and subsequent lecture.

Permission to publish the information related to the Case Study by Williams is gratefully acknowledged.

REFERENCES

1. Turner, W.J. and Simonson, M.J., “Compressor Station Transient Flow Modeled”, Oil and Gas Journal 79-83, May 20, 1985.
2. Botros, K.K.: "Transient Phenomena in Compressor Stations During Surge", 37th ASME International Gas Turbine and Aeroengine Congress and Exposition, Cologne, Germany, June 1 - 4, 1992, also appeared in the J. of Eng. for Gas Turbine and Power, vol. 116, pp. 133-142, January, 1994.
3. Botros, K.K., Campbell, P.J. & Mah, D.B.: “Dynamic Simulation of Compressor Station Operation Including Centrifugal Compressor & Gas Turbine”, ASME Journal of Engineering for Gas Turbines and Power, Vol. 113, pp. 300-311, April, 1991.
4. Murphy, K.M., et al.: “On Modelling Centrifugal Compressors for Robust Control Design’, Int. Gas Turbine and Aeroengine Congress and Exposition, Cologne, Germany, 92-GT-231, June 1-4, 1992.
5. Paltovany, D. and Focke, A.B., “Predictive Surge Control Optimization for A Centrifugal Compressor”, J. of Turbomachinery, Vol. 108, 82- 89, July, 1986.
6. Botros, K.K., Jones, J.B. & Roorda, O.: “Flow Characteristics and Dynamics of Swing Check Valves In Compressible Flow Applications - Part I”, 1996 ASME Pressure Vessels and Piping Conference, Symposium on Fluid Structure Interaction, Montreal, Quebec, Canada, PVP-Vol. 337, pp.241-250, July 21-26, 1996.
7. Wylie, E.B., Streeter, V.L. & Stoner, M.A.: “Unsteady-State Natural Gas Calculations in Complex Pipe Systems”, Society of Petroleum Engineering Journal, pp. 35- 43, Feb., 1974.
8. Moore, J.J., Kurz, R., Garcia-Hernandez, A., Brun, K.: “Experimental evaluation of the transient behavior of a compressor station during emergency shutdowns”, ASME Turbo Expo, Orlando, FL., June 8-12, 2009.
9. Nored, M.G., Brun, K., Kurz, R.: “Development of a guideline for the design of surge control systems”, ASME Turbo Expo, Berlin; June 9-13, 2008.
10. SchjØlberg, I., Hyllseth, M., Skofteland, G., Nordhus, H., Dynamic analysis of compressor trips in the SnØhvit LNG refrigerant circuits, ASME Turbo Expo, Berlin; June 9-13, 2008.
11. Locke, S.R.: An Empirical Solution to an Anti-surge Control Problem”, Proceedings of the 13th Turbomachinery Symposium, pp. 51-8, 1984. http://turbolab.tamu.edu/proc/turboproc/T13/index.html.
12. Botros, K.K. And D.J. Richards: "Analysis of the Effects Of Centrifugal Compressor’s Performance Characteristics During ESD", 11th Symposium On Industrial Applications Of Gas Turbines, Canadian Gas Association, Banff, Alberta, Canada, October 11-13, 1995.
13. Botros, K.K., Richards, D.J., Brown, R.J. and Stachniak, D.M.: "Effects Of Low Power Turbine/Compressor Rotor Inertia During Shutdown", Presented at the 1993 Symposium on the Industrial Application of Gas Turbines, Canadian Gas Association, Banff, Alberta, October 13 - 15, 1993.
14. Botros, K.K., Jungowski, W.M., And Richards, D.J.: "Compressor Station Recycle System Dynamics During Emergency Shutdown", ASME Transactions, J. Eng. for Gas Turbines and Power, Vol. 118, pp. 641-653, July, 1996.
15. Botros, K.K., B.J. Jones and D.J. Richards: "Recycle Dynamics during Centrifugal Compressor ESD, Startup and Surge Control", International Pipeline Conference (IPC), ASME, Calgary, Alberta, Canada, June 9-14, 1996.
16. Botros, K.K., Richards, D.J. and Roorda, O.: "Effect of Check Valve Dynamics On Sizing of Recycle Systems For Centrifugal Compressors", 41st ASME International Gas Turbine and Aeroengine Congress And Exposition (Turbo-Expo), Birmingham, UK, June 10-13, 1996.
17. White, R.C. and Kurz, R.: “Surge Avoidance for Compressor Systems”, Proceedings of the 35th Turbomachinery Symposium, George R. Brown Convention Center, Houston, Texas, 2006.
18. Botros, K.K.: "Single vs. Dual Recycle System Dynamics of High Pressure Ratio, Low Inertia Centrifugal Compressor Stations", ASME Journal of Engineering for Gas Turbines and Power, Volume 133, Issue 12, 12 pages, December 2011.
19. Greitzer, E.M.: “Surge And Rotating Stall in Axial Flow Compressors”, J. Of Eng. For Power, Transaction Of ASME, 190-198, April, 1976.
20. Moore, K.K. and Greitzer, E.M.: “A Theory of Post Stall Transients In Axial Compression Systems”, J. of Eng. For Gas Turbines and Power, Vol. 108, 68-76, 1986.
21. Botros, K.K. and Ganesan, S.T.: “Dynamic Instabilities in Industrial Compression Systems with Centrifugal Compressors”, Proceedings of the 37th Turbomachinery Symposium, George R. Brown Convention Center, Houston, Texas, September 8-11, 2008.
22. Botros, K.K. And Petela, G., "Use Of Method of Characteristics & Quasi-Steady Approach In Transient Simulation Of Compressor Stations", 1994 ASME Fluids Engineering Division Summer Meeting - Advances In Computational Methods In Fluid Dynamics, June 19 - 23, 1994, Lake Tahoe, Nevada, U.S.A., Fed - Vol. 196, Pp. 325 - 338.
23. Botros, K.K and Van Hardeveld, T.: “Pipeline Pumping and Compression Systems: A Practical Approach”, ASME Press, 2nd Edition, 2012.
24. Zucrow M.J. & Hoffman J.P.: Gas Dynamics, Vol. I, and Vol. II, John Wiley & Sons Inc., 1976.

25. Kentfiled, J.A.C.: Non-Steady, One-Dimensional, Internal, Compressible Flows – Theory and Applications, Oxford Science Publication, 1993.
26. Fox, J.A.: Hydraulic Analysis of Unsteady Flow In Pipe Networks, John Wiley & Sons Inc., 1977.
27. Osiadacz, A.: Simulation of Transient Gas Flows In Networks, Int. J. for Numerical Methods in Fluids, vol. 4, pp. 13-24,1984.
28. Shapiro, A.H.: The Dynamics and Thermodynamics of Compressible Fluid Flow – Vol. 2, E. Krieger Publishing Co., Malabar, Florida, pp. 972-973, 1983.
29. O. Kunz, R. Klimeck, W. Wagner and M. Jaeschke, "Groupe Européen de Recherches Gazières (GERG), Technical Monograph, GERG TM15.," 2007.
30. Courant, R., Friedrichs, K. and Lewy, H.: "On the partial difference equations of mathematical physics", IBM Journal, March 1967, pp. 215-234, English translation of the 1928 German original.